Hindawi
Journal of Mathematics
Volume 2020, Article ID 8890820, 14 pages
https://doi.org/10.1155/2020/8890820

Research Article

Study of Heat Transfer under the Impact of Thermal Radiation, Ramped Velocity, and Ramped Temperature on the MHD Oldroyd-B Fluid Subject to Noninteger Differentiable Operators

Syed Tauseef Saeed,[1] **Ilyas Khan**,[2] **Muhammad Bilal Riaz**,[3,4] **and Syed Muhammad Husnine**[1]

[1]*Department of Science & Humanities, National University of Computer and Emerging Sciences, Lahore Campus 54000, Lahore, Pakistan*
[2]*Department of Mathematics, College of Science Al-Zulfi, Majmaah University, Al-Majmaah 11952, Saudi Arabia*
[3]*Department of Mathematics, University of Management and Technology, Lahore 54000, Pakistan*
[4]*Institute for Groundwater Studies (IGS), University of the Free State, Bloemfontein 9301, South Africa*

Correspondence should be addressed to Syed Tauseef Saeed; tauseefsaeed301@gmail.com and Muhammad Bilal Riaz; bilal.riaz@umt.edu.pk

Received 20 September 2020; Revised 4 October 2020; Accepted 18 November 2020; Published 7 December 2020

Academic Editor: George Psihoyios

This theoretical study explores the impact of heat generation/absorption with ramp wall velocity and ramp wall temperature on the magnetohydrodynamic (MHD) time-dependent Oldroyd-B fluid over an unbounded plate embedded in a porous surface. The mathematical analysis of fractional governing partial differential equations has been established using systematic and powerful techniques of Laplace transform with its numerical inversion algorithms. The fractionalized solutions have been traced out separately through all fractional differential operators. Nondimensional parameters along with Laplace transformation are used to find the solution of temperature and velocity profiles. Fractional time derivatives are used to analyze the impact of fractional parameters (memory effect) on the dynamics of the fluid. While making a comparison, it is observed that the fractional-order model is the best to explain the memory effect as compared to classical models. The obtained solutions are plotted graphically for different values of physical parameters. Our results suggest that the velocity profile decreases by increasing the effective Prandtl number. Furthermore, the existence of an effective Prandtl number may reflect the control of the thickness of momentum and enlargement of thermal conductivity.

1. Introduction

The interest in studying problems involving non-Newtonian fluid flows has considerably grown for their wide range of applications: from drilling oil and gas wells and well completion operations to industrial processes involving waste fluids, synthetic fibre foodstuffs, and the extrusion of molten plastics. The attributes of fluid flow trace the diversity of the physical structure for non-Newtonian fluid flow. In such a fluid, stress and rate of strain have a nonlinear relationship. Oldroyd-B fluids have become a significant model of rate-type fluid. The procedure for the flow of rate-type fluids was discussed by Oldroyd [1]. Viscoelasticity has important implications due to the characterization of viscoelastic parameters (relaxation and retardation phenomenon), elastic shearing strain, thermal relaxation, and other rheological properties [2, 3]. In this regard, the thermodynamical analysis for the constitutive model of thermoplastic, viscoelastic, and viscoplastic was observed by Krairi and

Doghri [4] through the Cattaneo–Christov heat model. The temperature distribution and relaxation time of the heat flux were emphasized by the temperature equation.

The technique of fractional calculus has been used to formulate mathematical modeling in various technological developments, engineering applications, and industrial sciences. Different valuable work has been discussed for modeling fluid dynamics, signal processing, viscoelasticity, electrochemistry, and biological structure through fractional time derivatives. This fractional differential operator found useful conclusions for experts to treat cancer cells with a suitable amount of heat source and has compared the results to see the memory effect of the temperature function. As compared to classical models, the memory effect is much stronger in fractional derivatives. From the past to the present, modeling of different processes is handled through various types of fractional derivatives and fractal-fractional differential operators, such as Caputo (power law), Atangana–Baleanu (Mittag–Leffler law), Caputo–Fabrizio (exponential law), Riemann–Liouville, and modified Riemann–Liouville (power law with boundaries) [5–16]. Ramped wall velocity and temperature with MHD fluid flow are gaining attention of many researchers. Physically, the implementation of ramped wall velocity with temperature in real-life problems has a significant role, but mathematically, it is difficult to handle such conditions. Ramped heating is used to control and increase the temperature with adiabatic conditions in an effective way. Firstly, Ahmed and Dutta [17] discussed the simultaneous use of ramped velocity and ramped temperature. Seth et al. [18–20] investigated heat and mass transfer phenomena with ramp temperature conditions. Recently, Tiwana et al. [21] and Anwar et al. [22] analyzed the MHD Oldroyd-B fluid under the effect of ramped temperature and velocity.

In context with fractional differential operators, convective flow with ramped wall temperature for nonsingular kernel was analyzed by Riaz et al. [23]. Moreover, Riaz et al. [24] investigated the study of heat and mass transfer in the MHD Oldroyd-B fluid with ramped wall temperature using local and nonlocal differential operators. Additionally, the recent studies on modern fractional differential operators and viscoelastic fluids can be traced out in [25–38]. For this problem, the noninteger differentiable operator is chosen for the fractional MHD Oldroyd-B model which is developed under thermal radiation, ramp velocity, and ramp temperature associated with physical initial and boundary conditions. The model is solved via the Laplace transform technique and inversion algorithm. The required results are displayed in graphs with physical arguments.

2. Problem Statement

We discuss unsteady magnetohydrodynamic (MHD) fractional convective Oldroyd-B fluid flow under Boussinesq approximations over an infinite plate. Figure 1 represents the flow geometry of the magnetized Oldroyd-B fluid. Under these presumptions, the governing equation for the Oldroyd-B fluid with appropriate conditions is defined as follows [22]:

$$\left(1+\lambda_1\frac{\partial}{\partial\tau}\right)\frac{\partial w(\eta,\tau)}{\partial\tau}=\upsilon\left(1+\lambda_2\frac{\partial}{\partial\tau}\right)\frac{\partial^2 w(\eta,\tau)}{\partial\eta^2}-\left(1+\lambda_1\frac{\partial}{\partial\tau}\right)\frac{\sigma B_0^2}{\rho}w(\eta,\tau)+g\beta_T\left(1+\lambda_1\frac{\partial}{\partial\tau}\right)(T-T_\infty)-\left(1+\lambda_2\frac{\partial}{\partial\tau}\right)\frac{\mu\phi}{\rho k^*}w(\eta,\tau), \tag{1}$$

$$\left(\rho C_p\right)\frac{\partial T(\eta,\tau)}{\partial\tau}=\kappa\frac{\partial^2 T(\eta,\tau)}{\partial\eta^2}-\frac{\partial q_r}{\partial\eta}+Q_o\left(T-T_\infty\right). \tag{2}$$

The appropriate conditions are given as follows:

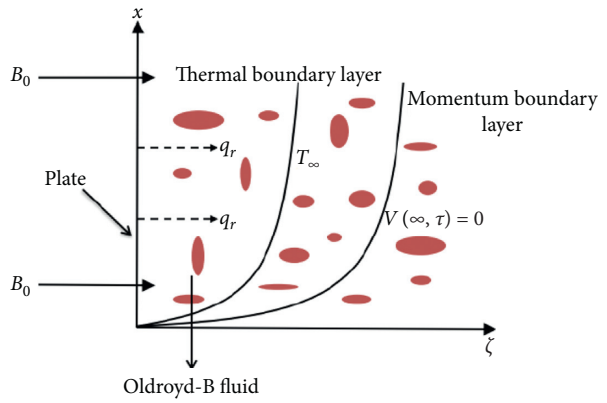

Figure 1: Geometrical presentation of the Oldroyd-B model.

$$
\begin{aligned}
&\tau > 0,\\
&w(\eta, 0) = 0,\\
&T(\eta, 0) = T_\infty,\\
&\frac{\partial w(\eta, 0)}{\partial \eta} = \frac{\partial w(\eta, 0)}{\partial \tau} = 0,\\
&\eta \geq 0,\\
&\tau > 0,\\
&w(0, t) = \begin{cases} U_o \dfrac{\tau}{\tau_o}, & \text{for } 0 < \tau < \tau_o;\\ U_o, & \text{for } \tau > \tau_o, \end{cases} \qquad (3)\\
&T(0, \tau) = \begin{cases} T_\infty + (T_w - T_\infty)\dfrac{\tau}{\tau_0}, & \text{for } 0 < \tau < \tau_o;\\ T_w, & \text{for } \tau > \tau_o, \end{cases}\\
&\tau > 0,\\
&w(\eta, \tau) \longrightarrow 0,\\
&T(\eta, \tau) \longrightarrow T_\infty,\\
&\text{as } \eta \longrightarrow \infty.
\end{aligned}
$$

The dimensionless parameters in equations (1) to (3) are mentioned in the following:

$$
\begin{aligned}
w &= \frac{V}{U_0},\\
\eta &= \frac{\zeta U_0}{v},\\
\tau &= \frac{t U_0^2}{v},\\
\tau_0 &= \frac{v}{U_0^2},\\
\theta &= \frac{T - T_\infty}{T_w - T_\infty},\\
\lambda_1 &= \frac{\lambda U_0^2}{v},\\
\lambda_2 &= \frac{\lambda_r U_0^2}{v},\\
P_r &= \frac{\mu C_p}{k},\\
Q &= \frac{v^2 Q_o}{\rho C_p U_0^2},\\
M &= \frac{\sigma B_0^2 v}{\rho U_0^2},\\
\frac{1}{K} &= \frac{\phi v^2}{k^* U_0^2}.
\end{aligned} \qquad (4)
$$

Applying (4) into (1)–(3), we required a set of dimensionless governing equations in the form of PDE's system presented as follows:

$$
\left(a_1 + \lambda \frac{\partial}{\partial \tau}\right)\frac{\partial V(\zeta, t)}{\partial t} = \left(1 + \lambda_r \frac{\partial}{\partial \tau}\right)\frac{\partial^2 V(\zeta, t)}{\partial \zeta^2} + \left(1 + \lambda \frac{\partial}{\partial \tau}\right) G_r \theta(\zeta, t) - a_2 V(\zeta, t), \qquad (5)
$$

$$
\frac{\partial \theta(\zeta, t)}{\partial t} = \frac{1}{P_{\text{reff}}}\frac{\partial^2 \theta(\zeta, t)}{\partial \zeta^2} + Q\theta(\zeta, t), \qquad (6)
$$

where $a_1 = 1 + \lambda M + (\lambda_r/K)$ and $a_2 = M + (1/K)$.

The dimensionless corresponding conditions can be given as follows:

$$\begin{aligned} &V(\zeta,0) = \theta(\zeta,0) = 0,\\ &V_t(\zeta,0) = V_\zeta(\zeta,0) = 0,\\ &\quad \text{for } \zeta \geq 0,\\ &\theta(0,t) = V(0,t) = \begin{cases} t, & \text{for } 0 < t < t_o,\\ 1, & \text{for } t > t_o, \end{cases}\\ &V(\zeta,\tau) \longrightarrow 0, \theta(\zeta,\tau) \longrightarrow 0, \quad \text{for } \zeta \longrightarrow \infty. \end{aligned} \tag{7}$$

2.1. Governing Equations in terms of Singular and Nonsingular Kernels. We define Caputo time derivative with its Laplace transform defined in the following [39]:

$$\begin{aligned} {}^{\mathrm{C}}D_t^{\kappa} g(\zeta,t) &= \frac{1}{\Gamma(n-\kappa)} \int_0^t \left(\frac{g^n(\tau)}{(t-\tau)^{\kappa+1-n}} \right) \mathrm{d}\tau,\\ L\left\{ {}^{\mathrm{C}}D_t^{\kappa} g(\zeta,t) \right\} &= s^{\kappa} L[g(\zeta,t)] - s^{\kappa-1} g(\zeta,0). \end{aligned} \tag{8}$$

The Caputo–Fabrizio fractional derivative and its Laplace transformation are defined as follows [40]:

$$\begin{aligned} {}^{\mathrm{CF}}D_t^{\kappa} g(\zeta,t) &= \frac{1}{(n-\kappa)} \int_0^t \exp\left(\frac{\kappa(1-\kappa)}{1-\kappa} \right) \frac{\partial g(\zeta,\tau)}{\partial \tau} \mathrm{d}\tau,\\ L\left\{ {}^{\mathrm{CF}}D_t^{\kappa} g(\xi,t) \right\} &= \frac{sL[g(\zeta,t)] - g(\zeta,0)}{(1-\kappa)s + \kappa}. \end{aligned} \tag{9}$$

The Atangana–Baleanu fractional derivative and its Laplace transformation are defined as follows [40]:

$$\begin{aligned} {}^{\mathrm{ABC}}D_t^{\kappa} g(\zeta,t) &= \frac{1}{(n-\kappa)} \int_0^t E_{\kappa}\left(\frac{\kappa(t-\kappa)^{\kappa}}{1-\kappa} \right) \frac{\partial g(\zeta,\tau)}{\partial \tau} \mathrm{d}\tau,\\ L\left\{ {}^{\mathrm{ABC}}D_t^{\kappa} g(\zeta,t) \right\} &= \frac{s^{\kappa} L[g(\zeta,t)] - s^{\kappa-1} g(\zeta,0)}{(1-\kappa)s^{\kappa} + \kappa}. \end{aligned} \tag{10}$$

3. Temperature Profile via Fractional Operators

3.1. Temperature Profile via the Caputo Approach. Generating equation (6) for the fractional form, we imposed equation (8) on equation (6), and we have

$${}^{\mathrm{C}}D_t^{\kappa} \theta(\zeta,t) = \frac{1}{P_{\mathrm{reff}}} \frac{\partial^2 \theta(\zeta,t)}{\partial \zeta^2} + Q\theta(\zeta,t). \tag{11}$$

We prefer to apply Laplace transform given in (8) on equation (11). The resultant form of the above expression is

$$\frac{\partial^2 \overline{\theta}(\zeta,p)}{\partial \zeta^2} - P_{\mathrm{reff}}\left(p^{\kappa} - Q\right) \overline{\theta}(\zeta,p) = 0. \tag{12}$$

The solution of equation (12) is

$$\overline{\theta}(\zeta,p) = c_1 e^{\zeta \sqrt{P_{\mathrm{reff}}\left(p^{\kappa}-Q\right)}} + c_2 e^{-\zeta \sqrt{P_{\mathrm{reff}}\left(p^{\kappa}-Q\right)}}, \tag{13}$$

and using equation (7), we find out the arbitrary parameter:

$$\overline{\theta}(\zeta,p) = \left(\frac{1-e^{-p}}{p^2} \right) e^{-\zeta \sqrt{P_{\mathrm{reff}}\left(p^{\kappa}-Q\right)}}. \tag{14}$$

3.2. Temperature Profile via the Caputo–Fabrizio Approach. Generating equation (6) for the fractional form, we imposed equation (9) on equation (6), and we have

$$\left(\frac{p}{(1-\kappa)p + \kappa} \right) \overline{\theta}(\zeta,p) = \frac{1}{P_{\mathrm{reff}}} \frac{\partial^2 \overline{\theta}(\zeta,p)}{\partial \zeta^2} + Q\overline{\theta}(\zeta,p), \tag{15}$$

$$\frac{\partial^2 \overline{\theta}(\zeta,p)}{\partial \zeta^2} - P_{\mathrm{reff}}\left(\frac{b_1 p + b_2}{b_3 p + b_4} \right) \overline{\theta}(\zeta,p) = 0. \tag{16}$$

The solution of equation (16) is

$$\overline{\theta}(\zeta,p) = c_1 e^{\zeta \sqrt{P_{\mathrm{reff}}\left(\left(b_1 p + b_2/b_3 p + b_4\right)\right)}} + c_2 e^{-\zeta \sqrt{P_{\mathrm{reff}}\left(\left(b_1 p + b_2/b_3 p + b_4\right)\right)}}, \tag{17}$$

and using equation (7), we find out the arbitrary parameter:

$$\overline{\theta}(\zeta,p) = \left(\frac{1-e^{-p}}{p^2} \right) e^{-\zeta \sqrt{P_{\mathrm{reff}}\left(\left(b_1 p + b_2\right)/\left(b_3 p + b_4\right)\right)}}. \tag{18}$$

3.3. Temperature Profile via the Atangana–Baleanu Approach. Generating equation (6) for the fractional form, we imposed equation (10) on equation (6), and we have

$$\left(\frac{p^{\kappa}}{(1-\kappa)p^{\kappa} + \kappa} \right) \overline{\theta}(\zeta,p) = \frac{1}{P_{\mathrm{reff}}} \frac{\partial^2 \overline{\theta}(\zeta,p)}{\partial \zeta^2} + Q\overline{\theta}(\zeta,p), \tag{19}$$

$$\frac{\partial^2 \overline{\theta}(\zeta,p)}{\partial \zeta^2} - P_{\mathrm{reff}}\left(\frac{b_1 p^{\kappa} + b_2}{b_3 p^{\kappa} + b_4} \right) \overline{\theta}(\zeta,p) = 0. \tag{20}$$

The solution of equation (20) is

$$\overline{\theta}(\zeta,p) = c_1 e^{\zeta \sqrt{P_{\mathrm{reff}}\left(\left(b_1 p^{\kappa} + b_2\right)/\left(b_3 p^{\kappa} + b_4\right)\right)}} + c_2 e^{-\zeta \sqrt{P_{\mathrm{reff}}\left(\left(b_1 p^{\kappa} + b_2\right)/\left(b_3 p^{\kappa} + b_4\right)\right)}}, \tag{21}$$

and using equation (7), we find out the arbitrary parameter:

$$\overline{\theta}(\zeta,p) = \left(\frac{1-e^{-p}}{p^2} \right) e^{-\zeta \sqrt{P_{\mathrm{reff}}\left(\left(b_1 p^{\kappa} + b_2\right)/\left(b_3 p^{\kappa} + b_4\right)\right)}}, \tag{22}$$

where $b_1 = 1 - Q + \kappa Q$, $b_2 = -\kappa Q$, and $b_3 = 1 - \kappa$, $b_4 = \kappa$.

4. Velocity Profile via Fractional Operators

4.1. Velocity Profile via the Caputo Approach. We utilize Laplace transformation for the solutions of the velocity profile given by equation (5):

$$\left(a_1+\lambda^{C}D_t^{\kappa}\right)\frac{\partial V(\zeta,t)}{\partial t}=\left(1+\lambda_r{}^{C}D_t^{\gamma}\right)\frac{\partial^2 V(\zeta,t)}{\partial \zeta^2}+\left(1+\lambda^{C}D_t^{\kappa}\right)G_rT(\zeta,t)-a_2V(\zeta,t). \tag{23}$$

We prefer to apply Laplace transform given in (8) on equation (23). The resultant form of the above expression is

$$\left(a_1+\lambda p^{\kappa}\right)p\overline{V}(\zeta,p)=\left(1+\lambda_r p^{\gamma}\right)\frac{\partial^2\overline{V}(\zeta,p)}{\partial\zeta^2}+\left(1+\lambda p^{\kappa}\right)G_r\overline{\theta}(\zeta,p)-a_2\overline{V}(\zeta,p). \tag{24}$$

The solution of the homogeneous part of (24) is

$$\overline{V}(\zeta,p)=c_1e^{\zeta\sqrt{\left(\left(\left(a_1+\lambda p^{\kappa}\right)p+a_2\right)/\left(1+\lambda_r p^{\gamma}\right)\right)}}+c_2e^{-\zeta\sqrt{\left(\left(\left(a_1+\lambda p^{\kappa}\right)p+a_2\right)/\left(1+\lambda_r p^{\gamma}\right)\right)}}. \tag{25}$$

The required solution can be written as

$$\overline{V}(\zeta,p)=c_1e^{\zeta\sqrt{\left(\left(\left(a_1+\lambda p^{\kappa}\right)p+a_2\right)/\left(1+\lambda_r p^{\gamma}\right)\right)}}+c_2e^{-\zeta\sqrt{\left(\left(\left(a_1+\lambda p^{\kappa}\right)p+a_2\right)/\left(1+\lambda_r p^{\gamma}\right)\right)}}-\frac{G_r\left(1+\lambda p^{\kappa}\right)\left(1-e^{-p}\right)e^{-\zeta\sqrt{P_{\text{reff}}\left(p^{\kappa}-Q\right)}}}{p^2\left[\left(P_{\text{reff}}\left(p^{\kappa}-Q\right)\right)\left(1+\lambda_r p^{\gamma}\right)-\left(\left(a_1+\lambda p^{\kappa}\right)p+a_2\right)\right]}, \tag{26}$$

$$\overline{V}(\zeta,p)=\left(\frac{1-e^{-p}}{p^2}\right)e^{-\zeta\sqrt{\left(\left(\left(a_1+\lambda p^{\kappa}\right)p+a_2\right)/\left(1+\lambda_r p^{\gamma}\right)\right)}}-\frac{G_r\left(1+\lambda p^{\kappa}\right)\left(1-e^{-p}\right)}{p^2\left[\left(P_{\text{reff}}\left(p^{\kappa}-Q\right)\right)\left(1+\lambda_r p^{\gamma}\right)-\left(\left(a_1+\lambda p^{\kappa}\right)p+a_2\right)\right]}\times\left\{e^{-\zeta\sqrt{\left(\left(\left(a_1+\lambda p^{\kappa}\right)p+a_2\right)/\left(1+\lambda_r p^{\gamma}\right)\right)}}-e^{-\zeta\sqrt{P_{\text{reff}}\left(p^{\kappa}-Q\right)}}\right\}. \tag{27}$$

4.2. Velocity Profile via the Caputo–Fabrizio Approach. We utilize Laplace transformation for the solutions of the velocity profile given by equation (5). We prefer to apply Laplace transform (9) on equation (5). The resultant form of the above expression is

$$\left(a_1+\lambda\left(\frac{p}{(1-\kappa)p+\kappa}\right)\right)p\overline{V}(\zeta,p)=\left(1+\lambda_r\left(\frac{p}{(1-\gamma)p+\gamma}\right)\right)\frac{\partial^2\overline{V}(\zeta,p)}{\partial\zeta^2}+\left(1+\lambda\left(\frac{p}{(1-\kappa)p+\kappa}\right)\right)G_r\overline{\theta}(\zeta,p)-a_2\overline{V}(\zeta,p). \tag{28}$$

The simplest form of the above equation is as follows:

$$\overline{V}(\zeta,p)=c_1e^{\zeta\sqrt{\left(\left(p+a_6\right)\left(\left(a_1p+a_8\right)p+a_2\right)\right)/\left(\left(p+a_4\right)\left(a_7p+a_6\right)\right)}}+c_2e^{-\zeta\sqrt{\left(\left(p+a_6\right)\left(\left(a_1p+a_8\right)p+a_2\right)\right)/\left(\left(p+a_4\right)\left(a_7p+a_6\right)\right)}}-\frac{G_r\left(p+a_6\right)\left(a_9p+a_4\right)\left(1-e^{-p}\right)}{p^2\left[P_{\text{reff}}\left(\left(a_3-Q\right)p+Qa_4\right)\left(a_7p+a_6\right)-\left(\left(p+a_6\right)\left(\left(a_1p+a_8\right)p+a_2\right)\right)\right]}\times e^{-\zeta\sqrt{P_{\text{reff}}\left(\left(\left(a_3-Q\right)p+Qa_4\right)/\left(p+a_4\right)\right)}}, \tag{29}$$

and using (7), we find out the arbitrary parameter:

$$\begin{aligned}\overline{V}(\zeta,p)=&\left(\frac{1-e^{-p}}{p^2}\right)e^{-\zeta\sqrt{(((p+a_6)((a_1p+a_8)p+a_2))/((p+a_4)(a_7p+a_6)))}}\\&-\frac{G_r(p+a_6)(a_9p+a_4)(1-e^{-p})}{p^2[P_{\text{reff}}((a_3-Q)p+Qa_4)(a_7p+a_6)-((p+a_6)((a_1p+a_8)p+a_2))]}\\&\times\left\{e^{-\zeta\sqrt{P_{\text{reff}}(((a_3-Q)p+Qa_4)/(p+a_4))}}-e^{-\zeta\sqrt{P_{\text{reff}}(((a_3-Q)p+Qa_4)/(p+a_4))}}\right\},\end{aligned}\tag{30}$$

where $a_1 = 1 + \lambda M + (\lambda_r/K)$, $a_2 = 1 + (M/K)$, $a_3 = (1/1-\kappa)$, $a_4 = (\kappa/1-\kappa)$, $a_5 = (1/(1-\gamma))$, $a_6 = (\gamma/(1-\gamma))$, $a_7 = 1 + a_5\lambda_r$, $a_8 = a_1a_4 + \lambda a_3$, and $a_9 = 1 + \lambda a_3$.

4.3. Velocity Profile via the Atangana–Baleanu Approach. We utilize Laplace transformation for the solutions of the velocity profile given by equation (5). We prefer to apply Laplace transform (10) on equation (5). The resultant form of the above expression is

$$\left(a_1+\lambda\left(\frac{p^\kappa}{(1-\kappa)p^\kappa+\kappa}\right)\right)p\overline{V}(\zeta,p)=\left(1+\lambda_r\left(\frac{p^\gamma}{(1-\gamma)p^\gamma+\gamma}\right)\right)\frac{\partial^2\overline{V}(\zeta,p)}{\partial\zeta^2}+\left(1+\lambda\left(\frac{p^\kappa}{(1-\kappa)p^\kappa+\kappa}\right)\right)G_r\overline{\theta}(\zeta,p)-a_2\overline{V}(\zeta,p),$$

$$\begin{aligned}\overline{V}(\zeta,p)=&\,c_1e^{\zeta\sqrt{(((p^\gamma+a_6)((a_1p^\kappa+a_8)p+a_2))/((p^\kappa+a_4)(a_7p^\gamma+a_6)))}}\\&+c_2e^{-\zeta\sqrt{(((p^\gamma+a_6)((a_1p^\kappa+a_8)p+a_2))/((p^\kappa+a_4)(a_7p^\gamma+a_6)))}}\\&-\frac{G_r(p^\kappa+a_6)(a_9p^\gamma+a_4)(1-e^{-p})}{p^2[P_{\text{reff}}((a_3-Q)p^\kappa+Qa_4)(a_7p^\gamma+a_6)-((p^\gamma+a_6)((a_1p^\kappa+a_8)p+a_2))]}\\&\times e^{-\zeta\sqrt{P_{\text{reff}}(((a_3-Q)p^\kappa+Qa_4)/((p^\kappa+a_4)))}},\end{aligned}\tag{31}$$

and using (7), we find out the arbitrary parameter:

$$\begin{aligned}\overline{V}(\zeta,p)=&\left(\frac{1-e^{-p}}{p^2}\right)e^{-\zeta\sqrt{(((p^\kappa+a_4)(a_7p^\gamma+a_6))/((p^\kappa+a_4)(a_7p^\gamma+a_6)))}}\\&-\frac{G_r(p^\kappa+a_6)(a_9p^\gamma+a_4)(1-e^{-p})}{p^2[P_{\text{reff}}((a_3-Q)p^\kappa+Qa_4)(a_7p^\gamma+a_6)-((p^\gamma+a_6)((a_1p^\kappa+a_8)p+a_2))]}\\&\times\left\{e^{-\zeta\sqrt{(((p^\gamma+a_6)((a_1p^\kappa+a_8)p+a_2))/((p^\kappa+a_4)(a_7p^\gamma+a_6)))}}-e^{-\zeta\sqrt{P_{\text{reff}}(((a_3-Q)p^\kappa+Qa_4)/((p^\kappa+a_4)))}}\right\}.\end{aligned}\tag{32}$$

As $\kappa \longrightarrow 1$, in the required velocity expressions (27), (30), and (32), we get the same result for the classical model as discussed in [22]. Furthermore, if we neglect $\lambda_1 = 0$ and $\lambda_2 = 0$, then the results are identical which were obtained by Riaz et al. [35]. This shows the validation of our obtained results. We use classical computational and numerical techniques such as Stehfest's [41] and Tzou's algorithms [42] for the inverse of

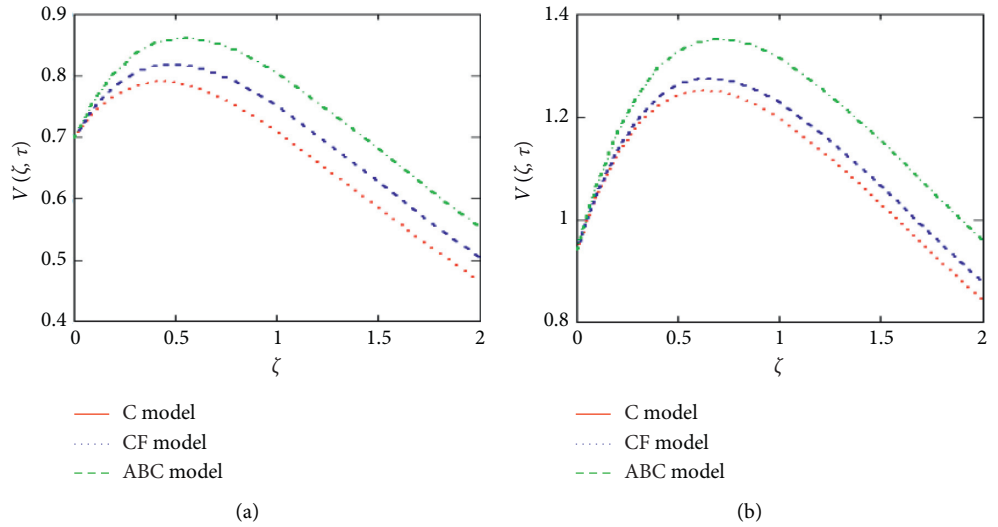

Figure 2: Comparison of the velocity profile for C, CF, and ABC with the variation of time.

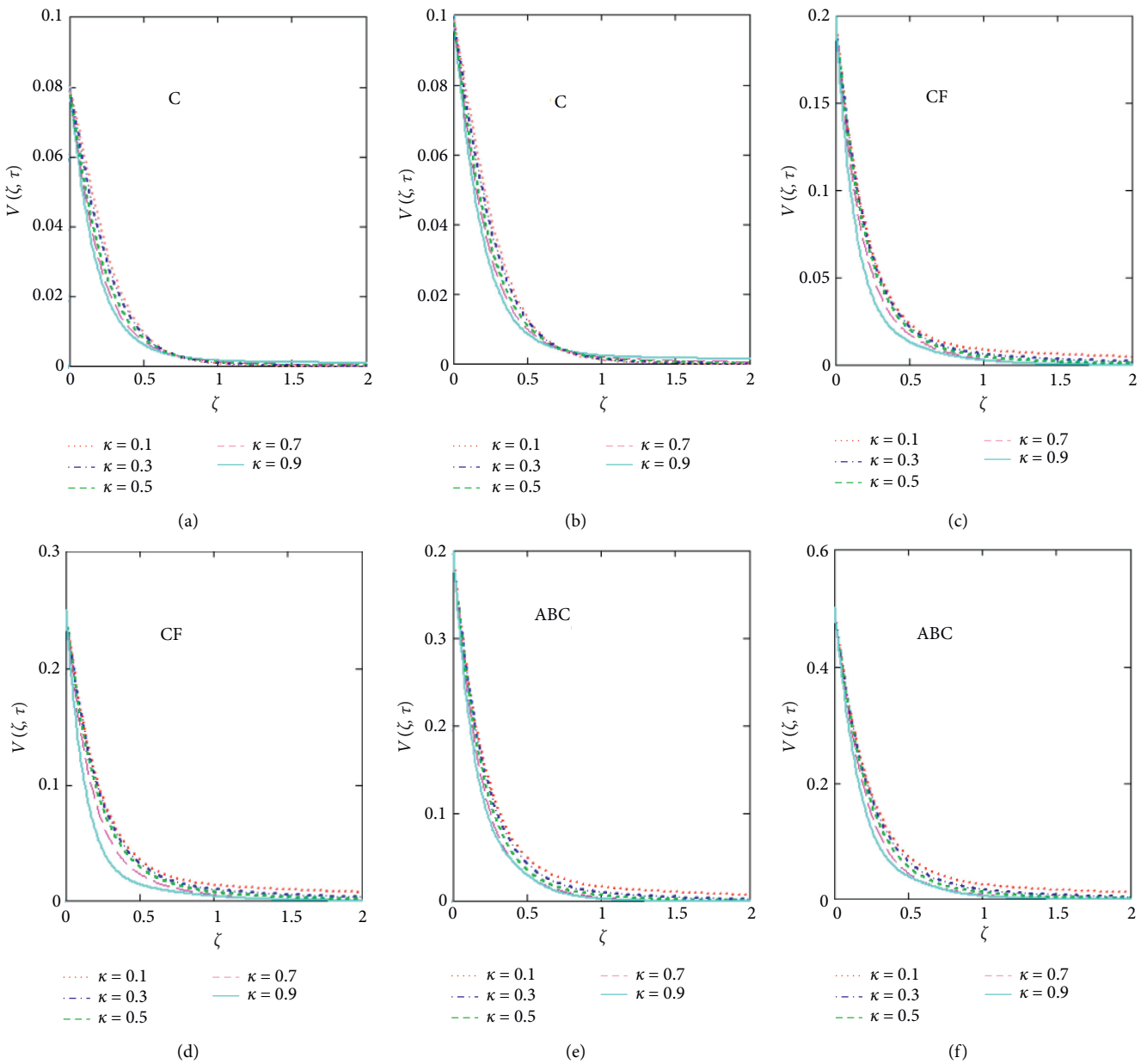

Figure 3: Plot via C, CF, and AB approaches for velocity with different values of κ.

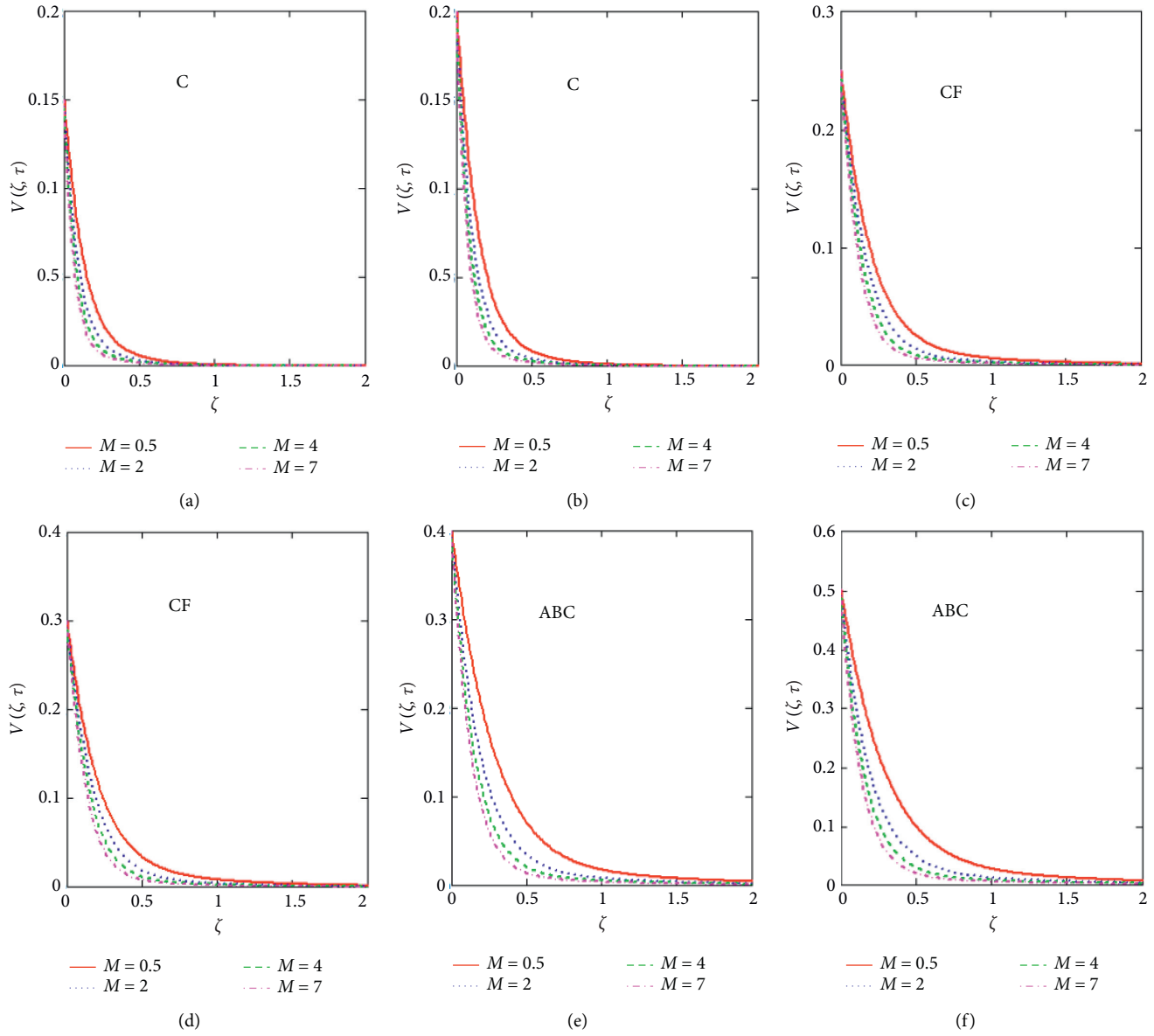

Figure 4: Plot via C, CF, and AB approaches for velocity with different values of M.

Laplace transform. Tzou's calculation for our numerical inverse Laplace is

$$v(r,t) = \frac{e^{4.7}}{t}\left[\frac{1}{2}\overline{v}\left(r,\frac{4.7}{t}\right) + R_e\left\{\sum_{k=1}^{N_1}(-1)^{\kappa}\overline{v}\left(r,\frac{4.7+k\pi i}{t}\right)\right\}\right], \tag{33}$$

where $R_e(\cdot)$ is the real part, i represents the imaginary part, and N_1 is the natural number.

5. Results and Discussion

This section is dedicated to present physical interpretation of the obtained results via C, CF, and AB differential operators on the MHD fractional Oldroyd-B fluid over an infinite vertical plate on the porous medium. Analytical results are investigated via Laplace transformation with the inversion algorithm for velocity and energy profiles. The graphical representations are depicted for showing the influences of different physical parameters on velocity and temperature using the package of Mathcad-15. The time influence on all fractional derivative operators is analyzed in Figure 2. It clearly shows that, for the variation of time, the behavior of the velocity profile is the same. The resultant velocity of the ABC model is larger than the other fractional models.

Effect of κ: the influence of fraction parameter κ on velocity can been seen through Figure 3. Clearly, fluid velocity reduces with the increase in the fractional parameter for small and large time. It is worth mentioning that profiles for these are best to explain the history (memory) of the fluids. While making comparison, velocity for the Atangana–Baleanu model is

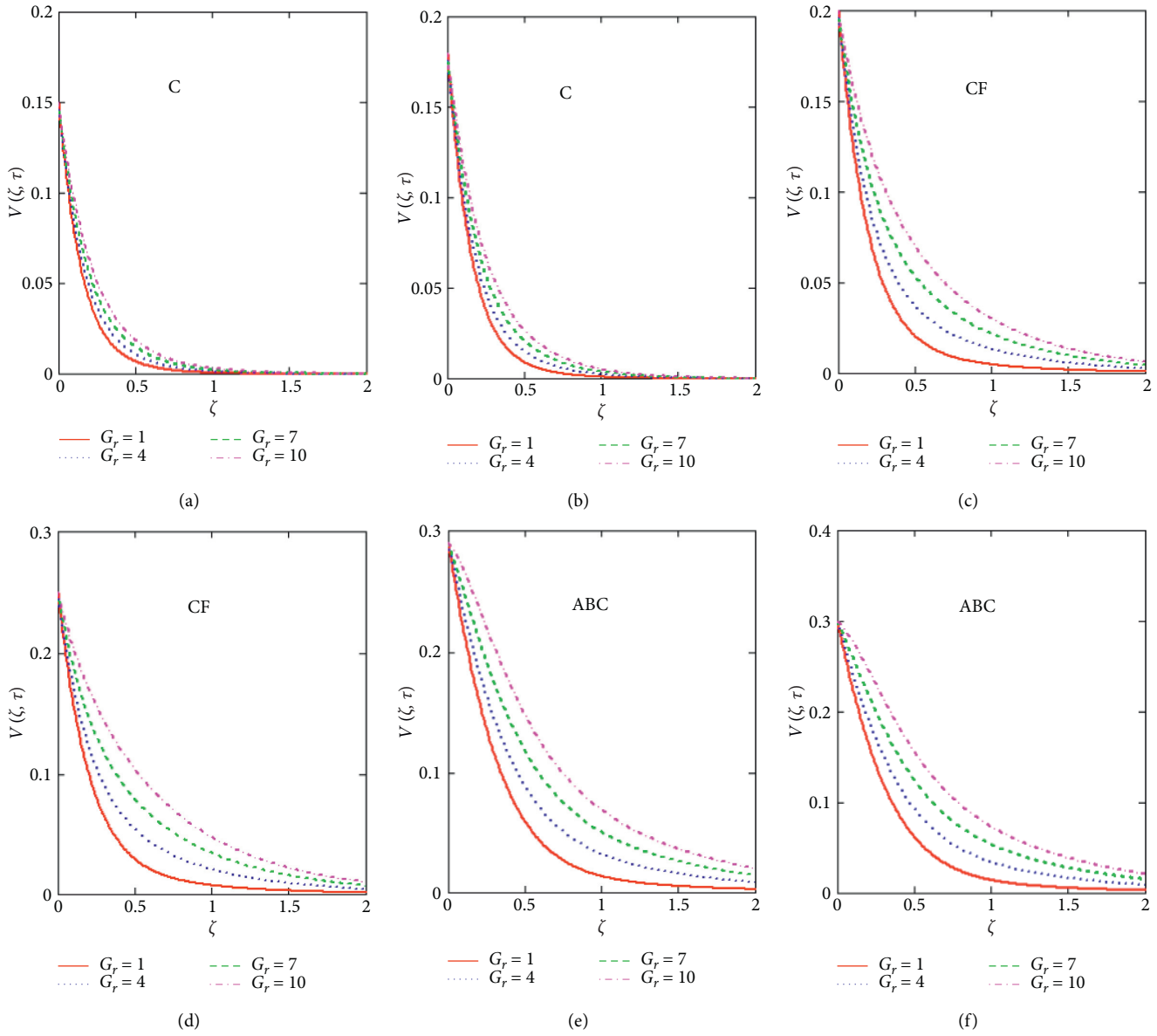

Figure 5: Plot via C, CF, and AB approaches for velocity with different values of G_r.

greatest because it has a nonlocal kernel. Velocity for CF is greater than C. This is because CF has a non-singular kernel that imitates C with the singular kernel.

Effect of M: Figure 4 investigates the impact of the magnetic force on all fractional operators. This graphical representation indicates that, with an increase in the magnetic field, the velocity reduces due to Lorentz force. By increasing the parameter of M, the Lorentz force also increases. Fluid flow on the boundary layer slows down due to this force.

Effect of G_r: Figure 5 shows the impact on G_r for the velocity field versus time. It can be seen that the velocity field enhances by increasing G_r. It is supported by the physical fact that G_r is the fraction of buoyancy and viscous forces. An increase in G_r means that the buoyancy force gets stronger near the plate such that it overcomes the viscous force and that the fluid gets accelerated.

Effect of λ: Figure 6 shows the impact on the velocity field for λ. As λ increases, the thickness of the momentum boundary layer reduces which results in the deceleration of the fluid. As a relaxation time increment implies that the fluid will take extra time to calm, it readily justifies the decrease in velocity. It is quite a reverse behavior as compared to λ_r.

Effect of λ_r: Figure 7 shows the behavior of velocity curves for λ_r. It is observed that velocity enhances with the increase in λ_r for all fractional models. The velocity behavior is also observed for the variation of time.

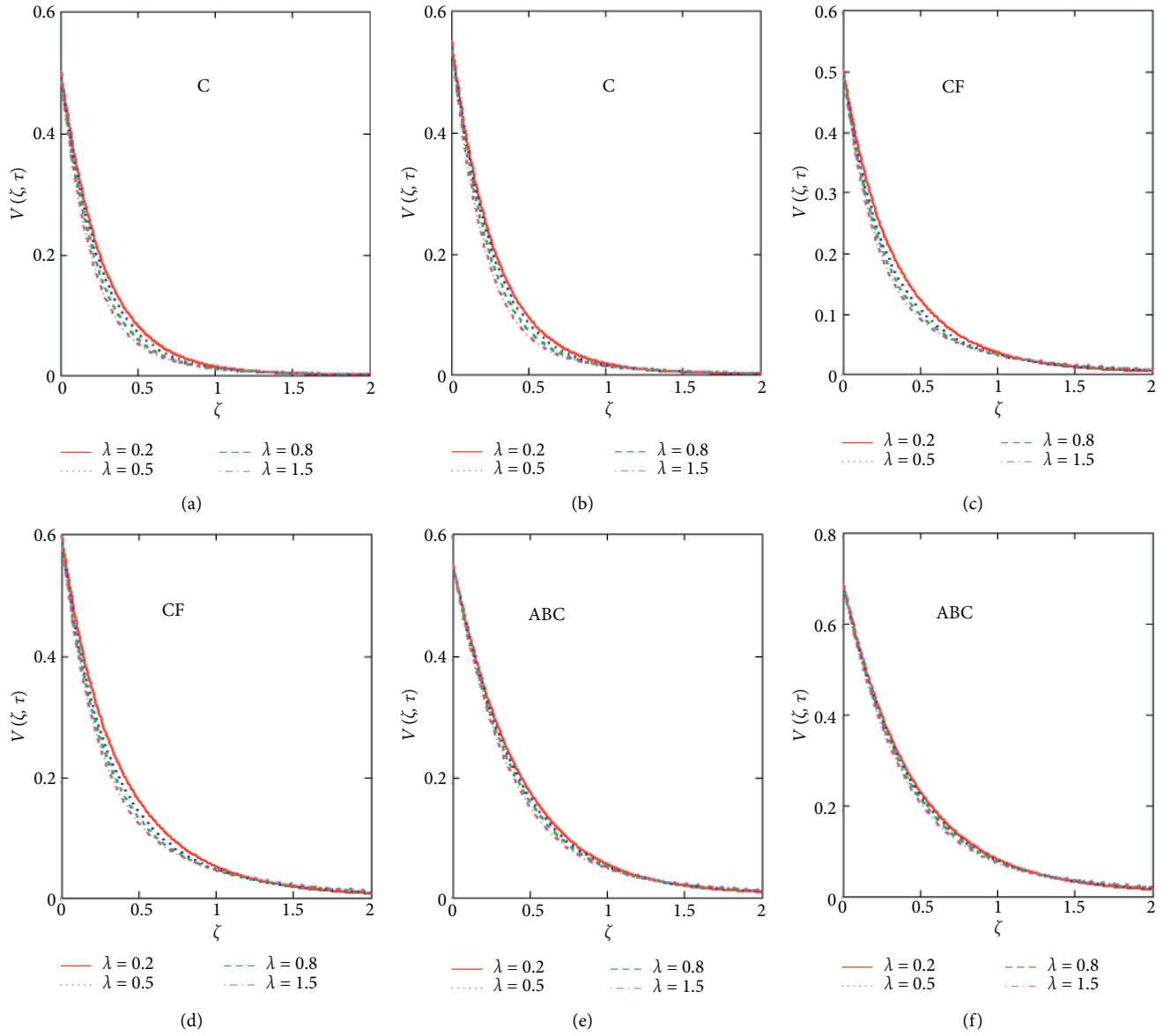

Figure 6: Plot via C, CF, and AB approaches for velocity with different values of λ.

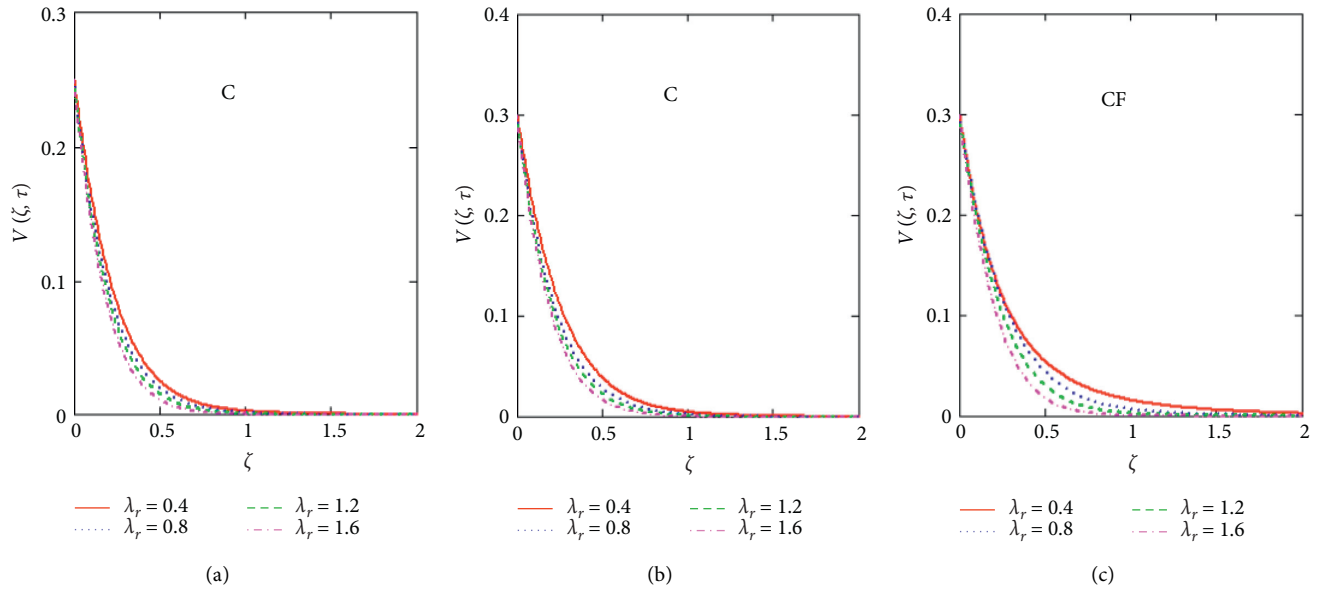

Figure 7: Continued.

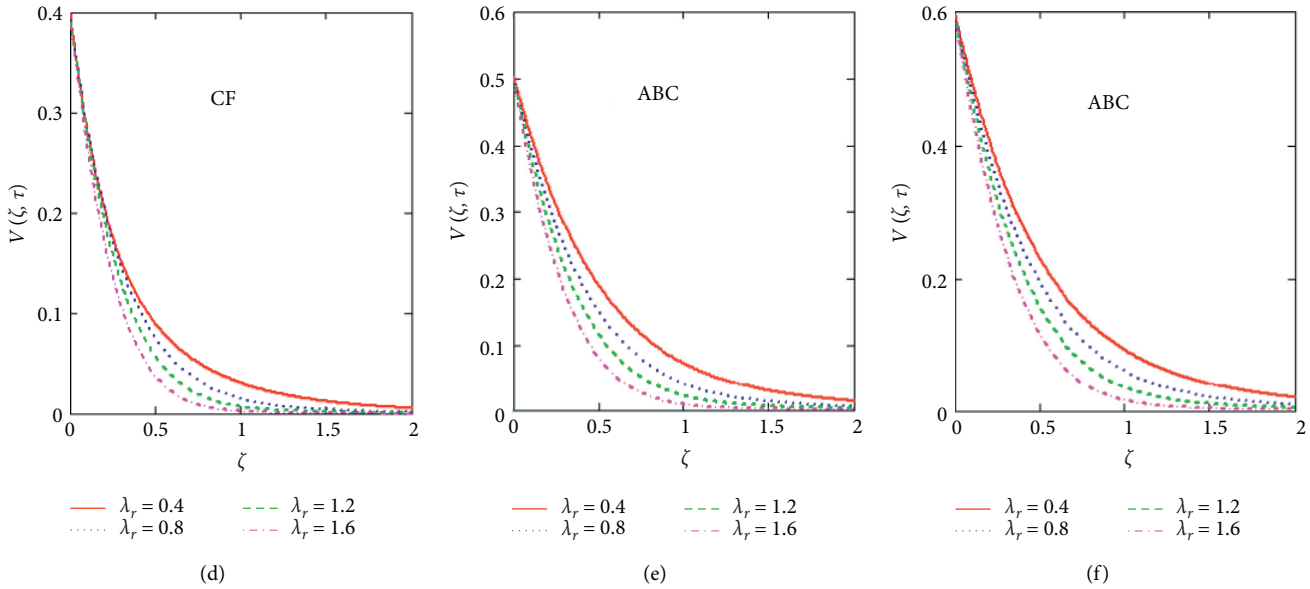

FIGURE 7: Plot via C, CF, and AB approaches for velocity with different values of λ_r.

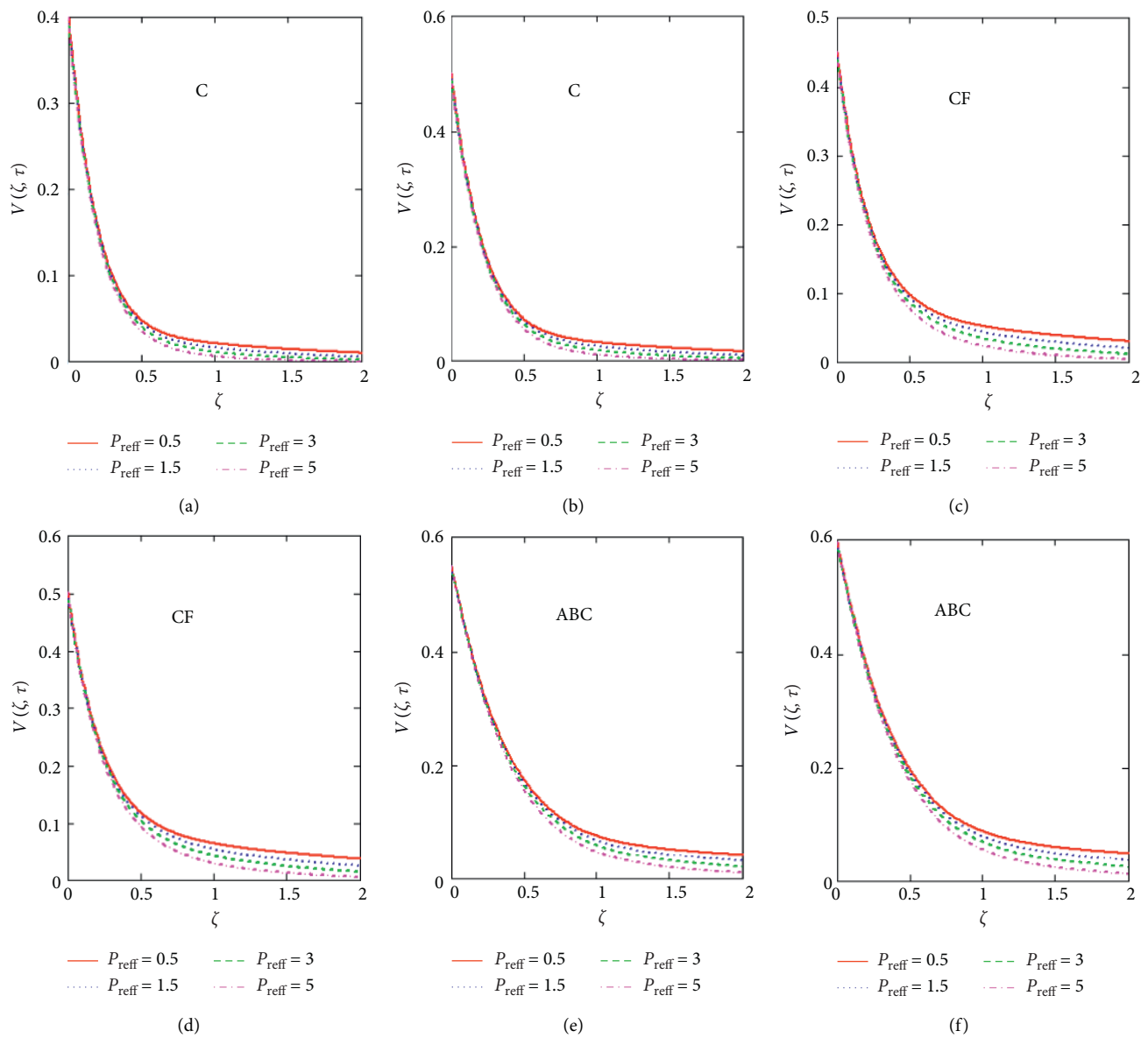

FIGURE 8: Plot via C, CF, and AB approaches for velocity with different values of P_{reff}.

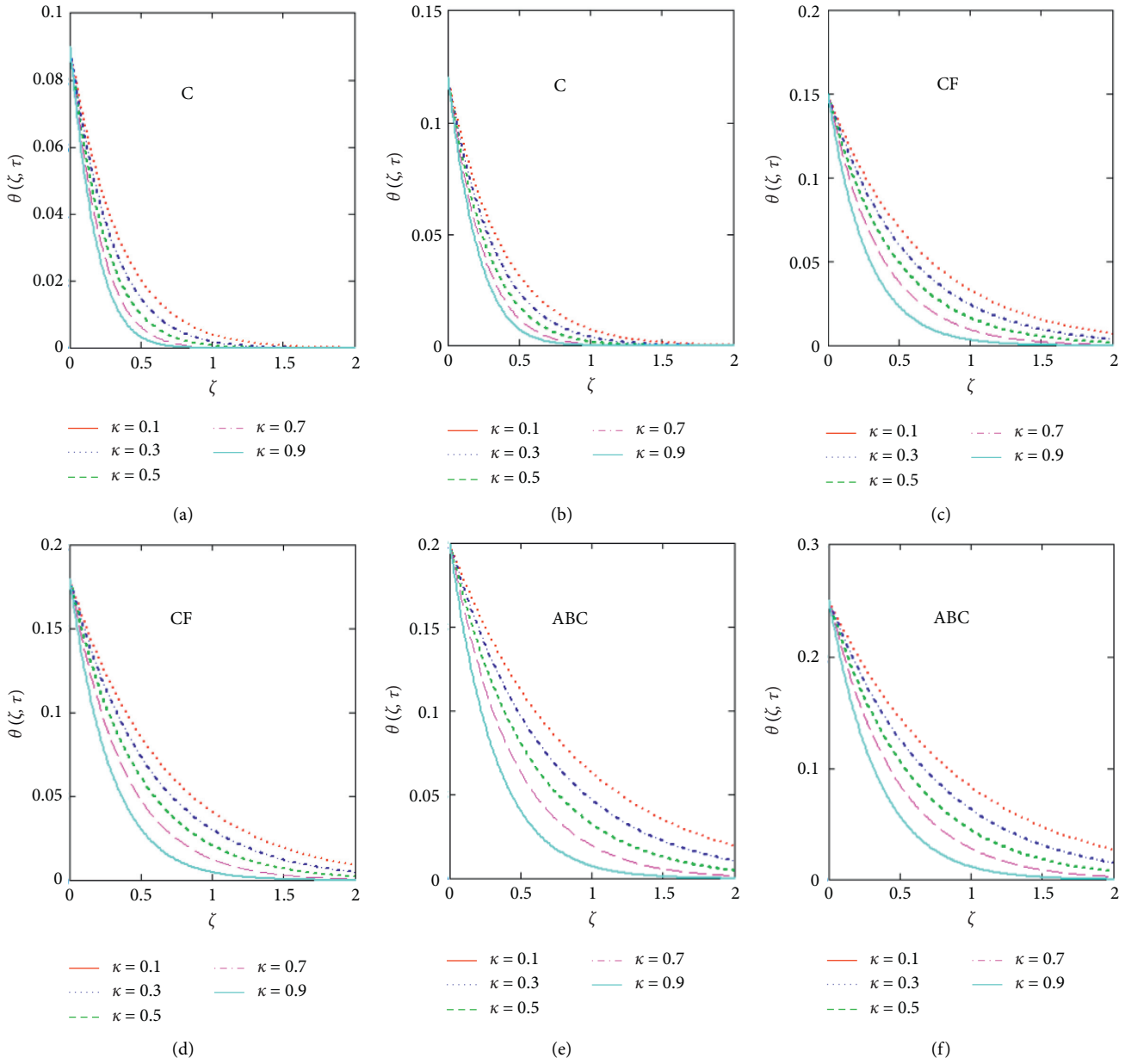

Figure 9: Plot via C, CF, and AB approaches for the temperature profile with different values of κ.

Effect of P_{reff}: Figure 8 discusses the effect of P_{reff} using C, CF, and ABC models with the variation of time. Specific heat boundary thickness depends on P_{reff}. The thickness of the momentum and boundary layer is controlled by P_{reff}. It is seen from the graph that the decrease in the velocity is observed by the increase in the value of P_{reff}.

Effect of κ: Figure 9 highlights the effect of the fractional parameter on the temperature profile for fractional models. With the increase in κ, the resultant temperature decreases. Temperature for CF and ABC is more as compared to C in all cases. Moreover, as $\kappa \longrightarrow 1$, temperature curves for noninteger order approach integer order.

6. Conclusion

This paper studies MHD Oldroyd-B fluid flow with ramped wall temperature and velocity under the influence of the thermal radiation in a porous medium. Fractional derivative operators with the inversion algorithm are used to acquire the solution of velocity and temperature. The significant remarks for this article are as follows:

(1) Velocity curves show decreasing behavior for fractional parameters κ and M. The velocity field decreases by increasing the value of Pr.

(2) Velocity increases as G_r increases for all fractional models.

(3) Velocity profile is a decreasing function of P_{reff} for all fractional operators.

(4) Velocity profile shows an opposite behavior for λ_1 and λ_r for all fractional operators.

(5) Temperature decreases by enhancing the value of the fractional parameter.

(6) ABC fractional operator is more considerable as compared to all the other fractional operators.

Data Availability

The data that support the findings of this study are available from the corresponding author upon reasonable request.

Conflicts of Interest

The authors declare no conflicts of interest.

Authors' Contributions

All authors contributed equally and significantly to writing this manuscript.

Acknowledgments

The authors are highly thankful and grateful for the support provided by the Deanship of Scientific Research at Majmaah University under Project no. 1439-41.

References

[1] J. G. Oldroyd, "On the formulation of rheological equations of state," *Proceedings of the Royal Society of London. Series A. Mathematical and Physical Sciences*, vol. 200, no. 1063, pp. 523–541, 1950.

[2] J. J. Choi, Z. Rusak, and J. A. Tichy, "Maxwell fluid suction flow in a channel," *Journal of Non-Newtonian Fluid Mechanics*, vol. 85, no. 2-3, pp. 165–187, 1999.

[3] K. A. Abro and A. Atangana, "Role of non-integer and integer order differentiations on the relaxation phenomena of viscoelastic fluid," *Physica Scripta*, vol. 95, no. 3, Article ID 035228, 2020.

[4] A. Krairi and I. Doghri, "A thermodynamically-based constitutive model for thermoplastic polymers coupling viscoelasticity, viscoplasticity and ductile damage," *International Journal of Plasticity*, vol. 60, pp. 163–181, 2014.

[5] A. U. Awan, M. Ali, and K. A. Abro, "Electroosmotic slip flow of Oldroyd-B fluid between two plates with non-singular kernel," *Journal of Computational and Applied Mathematics*, vol. 376, Article ID 112885, 2020.

[6] K. A. Abro and M. A. Solangi, "Heat transfer in magneto-hydrodynamic second grade fluid with porous impacts using caputo-fabrizoi fractional derivatives," *Punjab University Journal of Mathematics*, vol. 49, no. 2, pp. 113–125, 2017.

[7] M. Saqib, I. Khan, Y.-M. Chu, A. Qushairi, S. Shafie, and K. Sooppy Nisar, "Multiple fractional solutions for magnetic bio-nanofluid using Oldroyd-B model in a porous medium with ramped wall heating and variable velocity," *Applied Sciences*, vol. 10, no. 11, p. 3886, 2020.

[8] K. A. Abro, M. Hussain, and M. M. Baig, "A mathematical analysis of magnetohydrodynamic generalized burger fluid for permeable oscillating plate," *Punjab University Journal of Mathematics*, vol. 50, no. 2, pp. 97–111, 2018.

[9] M. Saqib, S. Shafie, I. Khan, Y.-M. Chu, and K. S. Nisar, "Symmetric MHD channel flow of nonlocal fractional model of BTF containing hybrid nanoparticles," *Symmetry*, vol. 12, no. 4, p. 663, 2020.

[10] K. A. Abro, M. Hussain, and M. M. Baig, "Influences of magnetic field in viscoelastic fluid," *International Journal of Nonlinear Analysis and Applications*, vol. 9, no. 1, pp. 99–109, 2018.

[11] K. A. Abro, I. Khan, and A. Tassaddiq, "Application of Atangana-Baleanu fractional derivative to convection flow of MHD Maxwell fluid in a porous medium over a vertical plate," *Mathematical Modelling of Natural Phenomena*, vol. 13, no. 1, p. 1, 2018.

[12] M. Saqib, A. R. Mohd Kasim, N. F. Mohammad, D. L. Chuan Ching, and S. Shafie, "Application of fractional derivative without singular and local kernel to enhanced heat transfer in CNTs nanofluid over an inclined plate," *Symmetry*, vol. 12, no. 5, p. 768, 2020.

[13] I. Khan, S. T. Saeed, M. B. Riaz, K. A. Abro, S. M. Husnine, and K. S. Nisar, "Influence in a Darcy's medium with heat production and radiation on MHD convection flow via modern fractional approach," *Journal of Materials Research and Technology*, vol. 5, no. 9, pp. 10015–10030, 2020.

[14] B. Lohana, K. A. Abro, and A. W. Shaikh, "Thermodynamical analysis of heat transfer of gravity-driven fluid flow via fractional treatment: an analytical study," *Journal of Thermal Analysis and Calorimetry*, 2020.

[15] M. Saqib, H. Hanif, T. Abdeljawad, I. Khan, S. Shafie, and K. Sooppy Nisar, "Heat transfer in MHD flow of maxwell fluid via fractional Cattaneo-Friedrich model: a finite difference approach," *Computers, Materials & Continua*, vol. 65, no. 3, pp. 1959–1973, 2020.

[16] K. A. Abro, I. Khan, and J. F. Gomez-Aguilar, "A mathematical analysis of a circular pipe in rate type fluid via Hankel transform," *European Physical Journal*, vol. 397, pp. 133–139, 2018.

[17] N. Ahmed and M. Dutta, "Transient mass transfer flow past an impulsively started infinite vertical plate with ramped plate velocity and ramped temperature," *International Journal of Physical Sciences*, vol. 8, pp. 254–263, 2013.

[18] G. Seth, R. Nandkeolyar, and M. S. Ansari, "Effect of rotation on unsteady hydromagnetic natural convection flow past an implusively moving vertical plate with ramped temperature in a porous medium with thermal diffusion and heat absorption," *International Journal of Applied Mathematics and Mechanics*, vol. 7, pp. 52–69, 2011.

[19] G. Seth, R. Sharma, and S. Sarkar, "Natural convection heat and mass transfer flow with Hall current, rotation, radiation and heat absorption past an accelerated moving vertical plate with ramped temperature," *Journal of Applied Fluid Mechanics*, vol. 8, pp. 7–20, 2015.

[20] G. S. Seth and S. Sarkar, "MHD natural convection heat and mass transfer flow past a time dependent moving vertical plate with ramped temperature in a rotating medium with hall effects, radiation and chemical reaction," *Journal of Mechanics*, vol. 31, no. 1, pp. 91–104, 2015.

[21] M. H. Tiwana, A. B. Mann, M. Rizwan et al., "Unsteady magnetohydrodynamic convective fluid flow of Oldroyd-B model considering ramped wall temperature and ramped wall velocity," *Mathematics*, vol. 7, no. 8, p. 676, 2019.

[22] T. Anwar, I. Khan, P. Kumam, and W. Watthayu, "Impacts of thermal radiation and heat consumption/generation on

unsteady MHD convection flow of an Oldroyd-B fluid with ramped velocity and temperature in a generalized darcy medium," *Mathematics*, vol. 8, no. 1, p. 130, 2019.

[23] M. B. Riaz, S. T. Saeed, D. Baleanu, and M. M. Ghalib, "Computational results with non-singular and non-local kernel flow of viscous fluid in vertical permeable medium with variant temperature," *Frontiers in Physics*, vol. 8, p. 275, 2020.

[24] M. B. Riaz, A. Atangana, and T. Abdeljawad, "Local and nonlocal differential operators: a comparative study of heat and mass transfers in mhd oldroyd-b fluid with ramped wall temperature," *Fractals*, vol. 28, no. 8, Article ID 2040033, 2020.

[25] K. A. Abro and A. Atangana, "A comparative study of convective fluid motion in rotating cavity via Atangana-Baleanu and Caputo-Fabrizio fractal-fractional differentiations," *European Physical Journal-Plus*, vol. 226, p. 135, 2020.

[26] K. A. Abro, "A fractional and analytic investigation of thermo-diffusion process on free convection flow: an application to surface modification technology," *European Physical Journal-Plus*, vol. 31, p. 135, 2020.

[27] M. B. Riaz and S. T. Saeed, "Comprehensive analysis of integer order, Caputo-Fabrizio and Atangana-Baleanu fractional time derivative for MHD Oldroyd-B fluid with slip effect and time dependent bounday conditions," *Discrete & Continuous Dynamical Systems*, 2020.

[28] S. T. Saeed, M. B. Riaz, D. Baleanu, and K. A. Abro, "A mathematical study of natural convection flow through a channel with non-singular kernels: an application to transport phenomena," *Alexandria Engineering Journal*, vol. 59, no. 4, pp. 2269–2281, 2020.

[29] M. M. Ghalib, A. A. Zafar, M. B. Riaz, Z. Hammouch, and K. Shabbi, "Analytical approach for the steady MHD conjugate viscous fluid flow in a porous medium with non-singular fractional derivative," *Physica A: Statistical Mechanics and its Applications*, vol. 554, Article ID 123941, 2019.

[30] D. Baleanu, S. Etemad, and S. Rezapour, "A hybrid caputo fractional modeling for thermostat with hybrid boundary value conditions," *Boundary Value Problems*, vol. 2020, no. 1, pp. 1–16, 2020.

[31] M. B. Riaz, "MHD Oldroyd-B fluid with slip condition in view of local and nonlocal kernels," *Journal of Applied and Computational Mechanics*, vol. 6, no. 1, pp. 1540–1551, 2020.

[32] M. B. Riaz, S. T. Saeed, and D. Baleanu, "Role of magnetic field on the dynamical analysis of second grade fluid: an optimal solution subject to non-integer differentiable operators," *Journal of Applied and Computational Mechanics*, vol. 6, no. SI, pp. 1475–1489, 2020.

[33] M. B. Riaz, A. Atangana, and S. T. Saeed, *MHD Free Convection Flow Over a Vertical Plate with Ramped Wall Temperature and Chemical Reaction in View of Non-singular Kernel*, Wiley, Hoboken, NJ, USA, 2020.

[34] N. Iftikhar, "Heat and mass transfer of natural convective flow with slanted magnetic field via fractional operators," *Journal of Applied and Computational Mechanics*, vol. 6, no. SI, pp. 1613–1636, 2020.

[35] M. B. Riaz, A. Atangana, and N. Iftikhar, "Heat and mass transfer in Maxwell fluid in view of local and non-local differential operators," *Journal of Thermal Analysis and Calorimetry*, 2020.

[36] R. Ahmad, A. Farooqi, J. Zhang, and N. Ali, "Steady flow of a power law fluid through a tapered non-symmetric stenotic tube," *Applied Mathematics and Nonlinear Sciences*, vol. 4, no. 1, pp. 255–266, 2019.

[37] A. Atangana and J. S. Gomez-Aguilar, "Decolonisation of fractional calculus rules: breaking commutativity and associativity to capture more natural phenomena," *European Physical Journal-Plus*, vol. 133, no. 4, p. 166, 2018.

[38] A. Atangana, "Non validity of index law in fractional calculus: a fractional differential operator with Markovian and non-markovian properties," *Physica A: Statistical Mechanics and its Applications*, vol. 505, pp. 688–706, 2018.

[39] M. Caputo and M. Fabrizio, "A new definition of fractional derivative without singular kernel," *Progress in Fractional Differentiation and Applications*, vol. 2, no. 1, pp. 1–11, 2016.

[40] A. Atangana and D. Baleanu, "New fractional derivatives with nonlocal and non-singular kernel: theory and application to heat transfer model," *Thermal Science*, vol. 20, no. 2, pp. 763–769, 2016.

[41] H. A. Stehfest, "Numerical inversion of Laplace transforms," *Communications of the ACM*, vol. 13, pp. 9–47, 1970.

[42] D. Y. Tzou, *Macro to Microscale Heat Transfer: The Lagging Behaviour*, Taylor & Francis, Washington, DC, USA, 1970.